Titre: Title:	Bayesian dynamic linear models for structural health monitoring
Auteurs: Authors:	James Alexandre Goulet
Date:	2017
Type:	Article de revue / Article
Référence: Citation:	Goulet, J. A. (2017). Bayesian dynamic linear models for structural health monitoring. Structural Control and Health Monitoring, 24(12), e2035. https://doi.org/10.1002/stc.2035

Document en libre accès dans PolyPublie
Open Access document in PolyPublie

URL de PolyPublie: PolyPublie URL:	https://publications.polymtl.ca/2647/
Version:	Version finale avant publication / Accepted version Révisé par les pairs / Refereed
Conditions d'utilisation: Terms of Use:	CC BY-NC-ND

Document publié chez l'éditeur officiel
Document issued by the official publisher

Titre de la revue: Journal Title:	Structural Control and Health Monitoring (vol. 24, no. 12)
Maison d'édition: Publisher:	Wiley
URL officiel: Official URL:	https://doi.org/10.1002/stc.2035
Mention légale: Legal notice:	This is the peer reviewed version of the following article: Goulet, J. A. (2017). Bayesian dynamic linear models for structural health monitoring. Structural Control and Health Monitoring, 24(12), e2035. https://doi.org/10.1002/stc.2035, which has been published in final form at https://doi.org/10.1002/stc.2035. This article may be used for non-commercial purposes in accordance with Wiley Terms and Conditions for Use of Self-Archived Versions. This article may not be enhanced, enriched or otherwise transformed into a derivative work, without express permission from Wiley or by statutory rights under applicable legislation. Copyright notices must not be removed, obscured or modified. The article must be linked to Wiley's version of record on Wiley Online Library and any embedding, framing or otherwise making available the article or pages thereof by third parties from platforms, services and websites other than Wiley Online Library must be prohibited.

Bayesian Dynamic Linear Models for Structural Health Monitoring

JAMES-A. GOULET[1]

[1]Department of Civil, Geologic and Mining Engineering

POLYTECHNIQUE MONTREAL, CANADA

May 22, 2017

Abstract

In several countries, infrastructure is in poor condition and this situation is bound to remain prevalent for the years to come. A promising solution for mitigating the risks posed by ageing infrastructure is to have arrays of sensors for performing, in real-time, *structural health monitoring* (SHM) across populations of structures. This paper presents a Bayesian Dynamic Linear Model (BDLM) framework for modeling the time-dependent responses of structures and external effects by breaking it into components. The specific contributions of this paper are to provide (1) a formulation for simultaneously estimating the hidden states of structural responses as well as the external effects it depends on, e.g. temperature and loading, (2) a state estimation formulation that is robust toward the errors caused by numerical inaccuracies, (3) an efficient way for learning the model parameters, and (4) a formulation for handling non-uniform time steps.

Keywords: Structural Health Monitoring (SHM), Bayesian models, Dynamic Lineal Models, Kalman Filter, Bridge, infrastructure

1 Introduction

In several countries, infrastructure is in poor condition and this situation is bound to remain prevalent for the years to come. A promising solution for mitigating the risk posed by ageing infrastructure is to have arrays of sensors deployed across cities to monitor, in real-time, the condition of infrastructure. We now have the technological capacity to measure and store the data for thousands of structures. However, *what is holding back SHM is that there is currently no generic and robust*

way to interpret the data collected by sensors. Many authors have approached this challenge using probabilistic methods such as response surfaces [9], ARX [2], ARMA [35], and Kalman-filter based methods [15, 28]. Other have approached the damage detection problem using pattern-recognition techniques [25] and Dynamic Bayesian Networks [1]. Another active sub-field is dedicated to the design of sensors systems themselves [4, 7, 10]. In their books, Yuen [31] and Farrar and Worden [11] present several Bayesian methods applied to SHM applications.

A key challenge remaining for enabling large-scale applications of SHM is to identify from time-series, the baseline response of structures without the effect of external actions such as temperature and traffic. To succeed at this task, a methodology must be able to operate seamlessly in conditions with frequent outliers and missing data. This paper proposes a framework for modeling the time-dependent responses of structures by breaking it into generic components, each having its own specific mathematical formulation. This new framework is a generalization of *Bayesian Dynamic Linear Models* (*BDLM*) for the field of structural health monitoring (SHM).

*BDLM*s are issued from the field of applied statistics where it is extensively used in business and finance applications [29, 30]. The theory behind *BDLM* comes from the field of control where took place the development of the Kalman filter for the control system of the Apollo mission [14]. In the field of Machine Learning, *BDLM*s are commonly referred to as *state-space models* [18]. In civil engineering, several examples of applications involving the Kalman filter with structural dynamic models are published in the field of SHM, [5, 6, 8, 17, 20, 24, 27, 28]. A first attempt to employ a *BDLM* for Structural Health Monitoring was presented by Solhjell [26]. Solhjell introduced many new concepts of *BDLM* to the field of SHM, yet, several key aspects are missing for enabling the general applications on civil structures.

This paper presents a framework employing Bayesian Dynamic Linear Models which is capable of estimating hidden state variables using time-discrete monitoring data of a structural response. Here, the term *hidden* refers to variables that are indirectly observed and *structural responses* refers to the behaviour of a structure such as its frequencies, displacement, strains, etc. Part of the contribution of this paper is to regroup in a holistic framework, the theories found in the fields of Machine learning [13, 18] and applied statistics [26, 29, 30]. This framework enables the general application of *BDLM* for the specific challenges encountered in SHM applications. The specific contributions of this paper are to provide:

1. a formulation for simultaneously estimating the hidden states of structural responses as well as the external effects it depends on, e.g. temperature and loading

2. a state estimation formulation that is robust toward the errors caused by

numerical inaccuracies

3. an efficient way for learning the parameters of the model

4. a formulation for handling non-uniform time steps

Section 2 presents the general formulation of the *BDLM* as well as the generic formulation for modelling each component involved in common SHM applications. Section 3 presents the general formulation behind the Kalman filter and Smoother that can be employed to estimate the hidden states of the model. This section also introduces the U-D filter that solves the numerical accuracy issues of the Kalman filter and smoother. Section 4 presents two Expectation Maximization formulation for learning the model parameters. Finally, Section 5 presents a simulated example showcasing the *BDLM*.

2 Bayesian Dynamic Linear Models

Bayesian Dynamic Linear Models (*BDLM*) are analogous to Hidden Markov Models (HMM) excepted that the states are Gaussian random variables, and the state transitions are defined by linear functions. The BDLM approach presented here aims at directly modeling the responses of a structure without requiring knowledge about its structural properties. Because it requires orders of magnitudes less structure-specific knowledge than what is required for building traditional finite element models, it is trivial to build a BDLM for any type of structure.

This section presents the general formulation of *BDLM*, the specificities of components modeling, the formulation for exact state estimation, a graphical representation for BDLMs and a procedure to handle non-uniform time steps.

2.1 *BDLM* formulation

In a *BDLM*, observations $\mathbf{y}_t$ at a time $t \in (1 : T)$ are modelled by superposing hidden states $\mathbf{x}_t$ from several generic components as defined by the observation model

$$\mathbf{y}_t = \mathbf{C}_t \mathbf{x}_t + \mathbf{v}_t, \quad \begin{cases} \mathbf{y}_t \sim \mathcal{N}(\mathbb{E}[\mathbf{y}_t], \mathrm{cov}[\mathbf{y}_t]) \\ \mathbf{x}_t \sim \mathcal{N}(\boldsymbol{\mu}_t, \boldsymbol{\Sigma_t}) \\ \mathbf{v}_t \sim \mathcal{N}(\mathbf{0}, \mathbf{R_t}) \end{cases} \tag{1}$$

where the *observation matrix* $\mathbf{C}_t$ indicates how each component from the hidden state vector $\mathbf{x}_t$ contribute to observations $\mathbf{y}_t$. The dynamic evolution of the hidden states $\mathbf{x}_t$ is described by the *transition model*

$$\mathbf{x}_t = \mathbf{A}_t \mathbf{x}_{t-1} + \mathbf{w}_t, \quad \{ \ \mathbf{w}_t \sim \mathcal{N}(\mathbf{0}, \mathbf{Q_t}). \tag{2}$$

In Equations (1) and (2) respectively, $\mathbf{v}_t$ denotes the Gaussian *measurement* errors with mean $\mathbf{0}$ and covariance $\mathbf{R_t}$, and $\mathbf{w}_t$ denotes the Gaussian *model* errors with mean $\mathbf{0}$ and covariance $\mathbf{Q_t}$. Note that when the model parameters are *stationary*, the index $_t$ can be dropped for matrices A, C, R and Q in Equations (1) and (2).

The *BDLM* serves three main purposes. A first purpose is to decompose a complex signal in its components by estimating the conditional probability of hidden state variables $\mathbf{x}_t$, given all observations up to the current time step t, $p(\mathbf{x}_t|\mathbf{y}_{1:t})$. In this paper, $p(\cdot|\cdot)$ denotes a conditional probability. A second purpose is to improve estimates of the structure behavior at a current time t, $p(\mathbf{y}_t|\mathbf{y}_{1:t})$, by combining the all the information obtained from observations up to t. A third purpose is to forecast the structure behavior at n time steps beyond the current time t, given all the information obtained up to t, $p(\mathbf{y}_{t+n}|\mathbf{y}_{1:t})$.

2.2 *BDLM* components for SHM

The key aspect of Bayesian Dynamic Linear Models is to represent the behavior of a system by superposing the effect of each of its hidden components. The term *hidden* means that a component is not directly observed. Figure 1 presents an example of raw structural responses recorded on a structure. In this illustrative example, the raw structural response is made of the superposition of several hidden components: (1) a local level (LL), (2) a cyclic temperature effect (S) and (3) an autoregressive error term (AR) to account for missing physical phenomena in the model. Subsections 2.2.1-2.2.4 present the formulation for modeling each common generic component that are useful for SHM applications. Note that each component is made of one or more hidden state variable. Here, the emphasis is put on the term *generic* because a vast array of structural behavior can be modelled by assembling combinations of the *generic components* presented in this section. The details about the derivation of this formulation is described by West and Harisson [30].

2.2.1 Local Level and Local Trend Components

The local level is a basic component that is found in almost every *BDLM*. It represents the evolution of the baseline response of the structure without the effect of external solicitations such as traffic loading or temperature. Analogously, a local level is employed to represent the average temperature and traffic loading. The local level generic formulation is defined by

$$\mathbf{x}^{\text{LL}} = x^{\text{LL}}, \ \mathbf{A}^{\text{LL}} = 1, \ \mathbf{C}^{\text{LL}} = 1, \ \mathbf{Q}^{\text{LL}} = (\sigma^{\text{LL}})^2$$

where the parameter σ^{LL} characterizes the model error term. This component is assumed to be *locally constant*, yet it can exhibit changes over time.
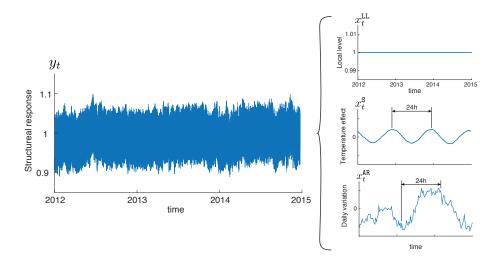
Figure 1: Example of raw structural response that is decomposed in three hidden components: (1) local level (LL), (2) cyclic temperature effect (S), and (3) an autoregressive error term (AR) to account for missing physical phenomena in the model.

Local trend components are suited for modeling a *locally constant* rate of change in the local level. Local trends are typically employed to model a drift over time in the response of structures. The generic formulation for the local trend is

$$\mathbf{x}^{\text{LT}} = \begin{pmatrix} x^{\text{LL}} \\ x^{\text{LT}} \end{pmatrix}, \ \mathbf{A}^{\text{LT}} = \begin{pmatrix} 1 & \Delta t \\ 0 & 1 \end{pmatrix}, \ \mathbf{C}^{\text{LT}} = \begin{pmatrix} 1 \\ 0 \end{pmatrix}, \ \mathbf{Q}^{\text{LT}} = (\sigma^{\text{LT}})^2 \begin{pmatrix} \frac{\Delta t^3}{3} & \frac{\Delta t^2}{2} \\ \frac{\Delta t^2}{2} & \Delta t \end{pmatrix}$$

where Δt is the time step size. In the transition matrix $\mathbf{A}^{\text{LT}}$, the first row adds to the local level the change cause by the local trend. The second row represents the locally constant trend. Analogously to the local level, over long periods, the local trend component can exhibit variation in the rate of change. In $\mathbf{C}^{\text{LT}}$ the 0 in the second row indicates that only the local level contributes to the observation y. $\mathbf{Q}^{\text{LT}}$ describes the effect of a variation in the rate of change, on the local level and local trend. Zarchan and Musoff [34] present the formulation for the *local acceleration* higher order model, and Mehrotra and Mahapatra [16] present the formulation for the *local jerk* model.

2.2.2 Periodic Components

Periodic components such as the daily variation ($p = 1$ day) and seasonal variation ($p = 365$ days) are described in their *Fourier form* by

$$\mathbf{x}^{\text{S}} = \begin{pmatrix} x^{\text{S1}} \\ x^{\text{S2}} \end{pmatrix}, \ \mathbf{A}^{\text{S}} = \begin{pmatrix} \cos \omega & \sin \omega \\ -\sin \omega & \cos \omega \end{pmatrix}, \ \mathbf{C}^{\text{S}} = \begin{pmatrix} 1 \\ 0 \end{pmatrix}, \ \mathbf{Q}^{\text{S}} = \begin{pmatrix} (\sigma^{\text{S1}})^2 & 0 \\ 0 & (\sigma^{\text{S2}})^2 \end{pmatrix}$$

5

where $\omega = \frac{2\pi \cdot \Delta t}{p}$, Δt is the time step length, and where x^{S1} corresponds to the amplitude of the periodic component. As indicated by the observation matrix $\mathbf{C}^{\text{S}}$, only the hidden state x^{S1} contributes to the observation y_t. For SHM applications, periodic components are suited to model daily and seasonal temperature variations which are described by two separated components. Note that this periodic component is not suited to model non-harmonic effects, for example such as those identified by Yuen and Kuok [32].

2.2.3 Autoregressive Components

The autoregressive component is suited to capture the dependence of the model errors between time steps. The dependence between model errors typically arises from missing physical phenomena in the *BDLM*. Although the AR components may contain several terms, the most common AR component includes only one term (AR(1)) so that

$$\mathbf{x}^{\text{AR}} = x^{\text{AR}}, \ \mathbf{A}^{\text{AR}} = \phi^{\text{AR}}, \ \mathbf{C}^{\text{AR}} = 1, \ \mathbf{Q}^{\text{AR}} = (\sigma^{\text{AR}})^2$$

This component exhibits two main regimes depending on the value of ϕ^{AR} [22]. For $0 < \phi^{\text{AR}} < 1$, the AR component is a stationary process with a fixed variance given by

$$(\sigma^{\text{AR},0})^2 = \frac{(\sigma^{\text{AR}})^2}{1 - (\phi^{\text{AR}})^2}.$$

For $\phi^{\text{AR}} \geq 1$, the AR component is a non-stationary process with no fixed value mean and variance. The special case where $\phi^{\text{AR}} = 1$ corresponds to a random walk. For most SHM applications, $0 < \phi^{\text{AR}} < 1$.

2.2.4 Regression Components

Regression components are employed to describe the dependencies between the state variables associated with different observations. In the context of SHM, regression components are employed to describe the dependencies between the response of a structure and the hidden state variables associated with temperature and traffic loading observations. Unlike other components previously presented, regression components are not defined by block component matrices. Instead, a regression component adds off-diagonal terms on the global observation matrix C. The relationship between the observation i and state variable j is taken into account by defining $[\mathbf{C}]_{ij} = \phi^{\text{i|j,R}}$ where $\phi^{\text{i|j,R}} \in \mathbb{R}$ is a regression coefficient.

2.3 Graphical Representation

Pearl [21] introduced graphical models, also known as Bayesian networks, as a general representation for the joint probability of random variables. Graphical

models combine the *theory of probabilities* with the *theory of graphs.* An example of trivial *BDLM* including only a local level is presented by a graphical model in Figure 2 where the graph in b) is a shorthand notation for the graph in a). In these graphical models, circles represent random variables; links correspond to causal relations; double-line links in the graph (b) are a shorthand notation for links between time steps in the graph (a). Color-filled nodes correspond to *observed variables*; white-filled nodes correspond to *unobserved/hidden variables.*
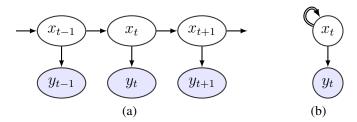

(a)   (b)

Figure 2: Graphical models describing (a) the expanded, (b) the compact graphical model representation of a trivial example of *BDLM* including only a local level component.

2.4 Non-uniform time steps

One challenge that arises while working with real data is that the time steps when data is recorded can be non-uniformly spaced. In order to accommodate non-uniform time steps, a reference time step Δt^{ref} must be defined. All parameter values in the parameter set $\mathcal{P}$ will be estimated for this reference time step. Parameter values for time steps that have a length Δt different than the reference value will have to be adapted.

For parameters associated with additive modeling error terms, i.e. model error standard deviations in $\mathbf{Q}$, it is proposed to scale σ proportionally to the ratio between the current time step and the reference time step so that

$$\sigma^{\Delta t} = \sigma^{\Delta t, \text{ref}} \frac{\Delta t}{\Delta t^{\text{ref}}}.$$

For the model transition matrix $\mathbf{A}$, the components associated with $\mathbf{A}^{\text{S}}$ and $\mathbf{A}^{\text{AR}}$ also need to be adapted. For $\mathbf{A}^{\text{S}}$, the time step Δt must be modified in the angular frequency term ω. $\mathbf{A}^{\text{AR}}$ contains the autoregressive coefficients that are recursively multiplied with the hidden state at each time step. To account for time step changes, autoregressive coefficients ϕ^{AR} are elevated to the power of the ratio between the current time step and the reference time step

$$\phi^{\text{AR},\Delta t} = \left(\phi^{\text{AR},\Delta t,\text{ref}}\right)^{\frac{\Delta t}{\Delta t^{\text{ref}}}}.$$

7

When a local trend component is employed, Δt should be adapted in $\mathbf{A}^{\mathrm{LT}}$. Note that the parameters in the observation matrix $\mathbf{C}$ and the measurement noise matrix $\mathbf{R}$ remain unchanged when the length of a time step is modified.

3 *BDLM* State Estimation: Kalman and U-D Filters/smoother

For a time series where $t = 1 : T$, the most common algorithms for estimating the hidden state variables are the *Kalman filter* (KF) and *Kalman smoother* (KS). The Kalman filter is suited for the online (i.e. in real-time) estimation of $p(\mathbf{x}_t|\mathbf{y}_{1:t})$, the hidden states at a time t given available observations $\mathbf{y}_{1:t}$.

The *Kalman filter* algorithm is commonly divided into the *prediction* and *measurement* steps.

Prediction step

$$
\begin{aligned}
p(\mathbf{x}_t|\mathbf{y}_{1:t-1}) &= \int \mathcal{N}(\mathbf{x}_t|\mathbf{A}_t\mathbf{x}_{t-1}, \mathbf{Q}_t)\mathcal{N}(\mathbf{x}_{t-1}|\boldsymbol{\mu}_{t-1}, \boldsymbol{\Sigma}_{t-1})d\mathbf{x}_{t-1} \\
&= \mathcal{N}(\mathbf{x}_t|\boldsymbol{\mu}_{t|t-1}, \boldsymbol{\Sigma}_{t|t-1}) \\
\boldsymbol{\mu}_{t|t-1} &\triangleq \mathbf{A}_t\boldsymbol{\mu}_{t-1} \\
\boldsymbol{\Sigma}_{t|t-1} &\triangleq \mathbf{A}_t\boldsymbol{\Sigma}_{t-1}\mathbf{A}_t^{\mathsf{T}} + \mathbf{Q}_t
\end{aligned}
\tag{3}
$$

Measurement step

$$
\begin{aligned}
p(\mathbf{x}_t|\mathbf{y}_{1:t}) &= \mathcal{N}(\mathbf{x}_t|\boldsymbol{\mu}_t, \boldsymbol{\Sigma}_t) && \\
\boldsymbol{\mu}_t &= \boldsymbol{\mu}_{t|t-1} + \mathbf{K}_t\mathbf{r}_t && \text{Posterior expected value} \\
\boldsymbol{\Sigma}_t &= (\mathbf{I} - \mathbf{K}_t\mathbf{C}_t)\boldsymbol{\Sigma}_{t|t-1} && \text{Posterior covariance} \\
\mathbf{r}_t &\triangleq \mathbf{y}_t - \hat{\mathbf{y}}_t && \text{Innovation vector} \\
\hat{\mathbf{y}}_t &\triangleq \mathbb{E}[\mathbf{y}_t|\mathbf{y}_{1:t-1}] = \mathbf{C}_t\boldsymbol{\mu}_{t|t-1} && \text{Prediction observations vector} \\
\mathbf{K}_t &\triangleq \boldsymbol{\Sigma}_{t|t-1}\mathbf{C}_t^{\mathsf{T}}\mathbf{S}_t^{-1} && \text{Kalman gain matrix} \\
\mathbf{S}_t &\triangleq \mathbf{C}_t\boldsymbol{\Sigma}_{t|t-1}\mathbf{C}_t^{\mathsf{T}} + \mathbf{R}_t && \text{Innovation covariance matrix}
\end{aligned}
\tag{4}
$$

The *Kalman gain* $\mathbf{K}_t$ represents the ratio between the prior covariance defined by the dynamic model and the measurement error covariance. If the variance of the prior knowledge is small (large) and the variance of the measurement errors large (small), the Kalman gain tends to one (zero). In the case of the posterior expected value, the Kalman gain is employed to weight the information coming from the prior $\boldsymbol{\mu}_{t|t-1}$ and the information coming from the observations, through the innovation vector $\mathbf{r}_t$.

The *Kalman smoother* is suited for offline estimation of the state at any time t given the entire time series $\mathbf{y}_{1:T}$. The Kalman smoother is initialized with the last step of the Kalman filter ($\boldsymbol{\mu}_{T|T}, \boldsymbol{\Sigma}_{T|T}$) and it propagates the information obtained for time steps $t : T$, on the state estimates for all previous time steps $1 : t - 1$. The Kalman smoother formulation follows

$$
\begin{aligned}
p(\mathbf{x}_t|\mathbf{y}_{1:T}) &= \mathcal{N}(\mathbf{x}_T|\boldsymbol{\mu}_{t|T}, \boldsymbol{\Sigma}_{t|T}) && \\
\boldsymbol{\mu}_{t|T} &= \boldsymbol{\mu}_{t|t} + \mathbf{J}_t(\boldsymbol{\mu}_{t+1|T} - \boldsymbol{\mu}_{t+1|t}) && \text{Posterior expected value} \\
\boldsymbol{\Sigma}_{t|T} &= \boldsymbol{\Sigma}_{t|t} + \mathbf{J}_t(\boldsymbol{\Sigma}_{t+1|T} - \boldsymbol{\Sigma}_{t+1|t})\mathbf{J}_t^\mathsf{T} && \text{Posterior covariance} \\
\mathbf{J}_t &\triangleq \boldsymbol{\Sigma}_{t|t}\mathbf{A}_{t+1}^\mathsf{T}\boldsymbol{\Sigma}_{t+1|t}^{-1} && \text{Backward Kalman gain matrix}
\end{aligned}
$$

(5)

Although the Kalman filter/smoother formulations presented in Equations (3) to (5) are the most widespread, it is also known to suffer from numerical instability issues [14], especially when:

1. The covariance is rapidly reduced in the measurement step, such as when extremely accurate measurements are used or when data is used after a long period where data was missing.

2. There is a large difference between the variance of several state variables contributing to the same observation.

For SHM applications, these cases are common and cause numerical instability issues. The U-D filter proposed by Bierman and Thornton [3] solves this issue by factorizing the covariance matrix using the Cholesky decomposition so that

$$
\boldsymbol{\Sigma}_t = \mathbf{U}_t\mathbf{D}_t\mathbf{U}_t^\mathsf{T}.
$$

Besides being numerically more stable, the U-D filter computes the same quantities, i.e. $p(\mathbf{x}_t|\mathbf{y}_{1:t})$ and has the same physical interpretation as the Kalman filter. Moreover it also has a comparable computational efficiency [14]. Because the formulation of the U-D filter is more involved than the one from the Kalman filter, the reader is invited to refer to specialized literature such as [14] and [23] for the complete formulation.

4   *BDLM* Parameter Estimation: EM Algorithm

A key aspect of *BDLM* is the estimation of model parameters for each component. One way of estimating parameters is to use an Expectation Maximisation (EM) algorithm.

9

E–step: Log-likelihood estimation using the Kalman smoother

The E in E-step stands for expectation. The estimation of model parameters requires the definition of a *performance metric* for the model. The conventional performance metric is the log-likelihood of observations. The log-likelihood of an observation is the logarithm of the prior probability of this observation at a time t, given our state estimate at time $t - 1$. Based on the hypothesis that all observations are independent, the log-likelihood is defined as

$$\ln p(\mathbf{y}_{1:T}) = \sum_{t=1}^{T} \ln \left(\mathcal{N}(\mathbf{y}_t | \mathbf{C}_t \boldsymbol{\mu}_{t|t-1}, \mathbf{S}_t) \right) \qquad (6)$$

where for the purpose of numerical accuracy, the product of the probabilities $\mathcal{N}(\mathbf{y}_t | \mathbf{C}_t \boldsymbol{\mu}_{t|t-1}, \mathbf{S}_t)$ is transformed as the sum of the log of probabilities. In the E-step, the log-likelihood is computed based on the state estimates $p(\mathbf{x}_t | \mathbf{y}_{1:t-1})$ obtained using a filtering algorithm.

M–step: Gradient Ascent

The M in M-step stands for maximization. The goal of the maximization step is to identify parameter values that maximize the log-likelihood estimated during a training period.

In this paper, two approaches are presented for the M-step, each having their strength and weaknesses. The first maximization scheme evaluates the derivative of the log-likelihood (see Eq.(6)) with respect to each matrix ($\mathbf{A}^{\text{old}}, \mathbf{C}^{\text{old}}, \mathbf{Q}^{\text{old}}, \mathbf{R}^{\text{old}}$) and sets it to zero to identify the new matrices ($\mathbf{A}^{\text{new}}, \mathbf{C}^{\text{new}}, \mathbf{Q}^{\text{new}}, \mathbf{R}^{\text{new}}$) that are maximizing the log-likelihood. Ghahramani and Hinton [13] have derived the analytical formulation resulting from the maximization operation so that

$$
\begin{aligned}
\mathbf{C}^{\text{new}} &= \left(\sum_{t=1}^{T} \mathbf{y}_t \boldsymbol{\mu}_t^{\mathsf{T}} \right) \left(\sum_{t=1}^{T} \boldsymbol{\Sigma}_t \right)^{-1} \\
\mathbf{R}^{\text{new}} &= \frac{1}{T} \sum_{t=1}^{T} \left(\mathbf{y}_t \mathbf{y}_t^{\mathsf{T}} - \mathbf{C}^{\text{new}} \boldsymbol{\mu}_t \mathbf{y}_t^{\mathsf{T}} \right) \\
\mathbf{A}^{\text{new}} &= \left(\sum_{t=2}^{T} \boldsymbol{\Sigma}_{t,t-1} \right) \left(\sum_{t=2}^{T} \boldsymbol{\Sigma}_{t-1} \right)^{-1} \qquad (7) \\
\mathbf{Q}^{\text{new}} &= \frac{1}{T-1} \left(\sum_{t=2}^{T} \boldsymbol{\Sigma}_t - \mathbf{A}^{\text{new}} \sum_{t=2}^{T} \boldsymbol{\Sigma}_{t,t-1}^{\mathsf{T}} \right) \\
\boldsymbol{\Sigma}_{t,t-1} &= (\mathbf{I} - \mathbf{K}_t \mathbf{C}_t)(\mathbf{A}_t \boldsymbol{\Sigma}_{t-1}).
\end{aligned}
$$

In addition to the model matrices, the initial hidden state can be updated following

$$
\begin{aligned}
\boldsymbol{\mu}_1^{\text{new}} &= \boldsymbol{\mu}_1 \\
\boldsymbol{\Sigma}_1^{\text{new}} &= \boldsymbol{\Sigma}_1 - \boldsymbol{\mu}_1 \boldsymbol{\mu}_1^{\mathsf{T}}.
\end{aligned}
\tag{8}
$$

Note that in Equations 7 & 8, $\boldsymbol{\mu}_t$ and $\boldsymbol{\Sigma}_t$ are estimated using a smoothing algorithm. The maximization operations presented in Equation (7) modifies simultaneously all terms in updated matrices ($\mathbf{A}^{\text{new}}, \mathbf{C}^{\text{new}}, \mathbf{Q}^{\text{new}}, \mathbf{R}^{\text{new}}$). It is thus necessary to replace specific terms that are not unknown parameters by the initial values in ($\mathbf{A}^{\text{old}}, \mathbf{C}^{\text{old}}, \mathbf{Q}^{\text{old}}, \mathbf{R}^{\text{old}}$). Optimizing simultaneously all the model matrices in order to maximize the log-likelihood has the upside to be fast and computationally efficient. However, this approach is also known for getting trapped in local maxima [19]. Because matrices $\mathbf{A}, \mathbf{C}, \mathbf{Q}, \mathbf{R}$ are typically sparse, modifying simultaneously all the terms in these matrices can lead to undesirable local maxima.

A second approach that can overcome this limitation is to perform the maximization with a parameter-wise approach instead of matrix-wise one. This maximization scheme employs a Newton-Raphson approach [12] where the first and second derivative of the log-likelihood (see Eq.(6)) with respect to each parameter θ_i enables to find new optimized parameter values so that

$$
\theta_i^{\text{new}} = \theta_i^{\text{old}} - \frac{\frac{\partial \ln p(\mathbf{y}_{1:T})}{\partial \theta_i}}{\frac{\partial^2 \ln p(\mathbf{y}_{1:T})}{\partial^2 \theta_i}}.
$$

Because this approach only optimizes the parameters of interest instead of entire matrices, it provides an additional tool in case the matrix-wise maximization is trapped in a local maximum.

The general procedure is to repeat the E and M steps recursively until the change in log-likelihood between iterations is below an admissible threshold. The main limitation of the EM algorithm is that it is only guaranteed to converge to a local maximum. This is an issue because the log-likelihood function is usually non-convex, which leads to several local maxima. One mitigation strategy is to use random initial parameter values to search for the region containing the global maximum.

5   Illustrative Example

An illustrative example showcases: (1) the construction of a BDLM, (2) model parameter estimation, (3) the separation of raw observations in generic components, and (4) the effect of missing data and outliers.

5.1 Simulated data

For the purpose of this example, simulated data is generated for representing a typical SHM application. The behavior of structures is often affected by temperature changes as well as traffic loading. Temperature variation is affected by a daily and a seasonal cycle. Traffic variation is affected by the daily traffic pattern. The structure's behavior that is simulated here is the first resonant frequency. All datasets are modelled for discrete time steps at intervals of 30 min (i.e. $\Delta t = \frac{1}{48}$ days/observations) for a total duration of two years so that $t = 1, 2, \cdots, T$; $T = 2 \times 365 \times 48$. Figure 3 presents the simulated observations generated for this example. The detailed procedure employed to generate simulated
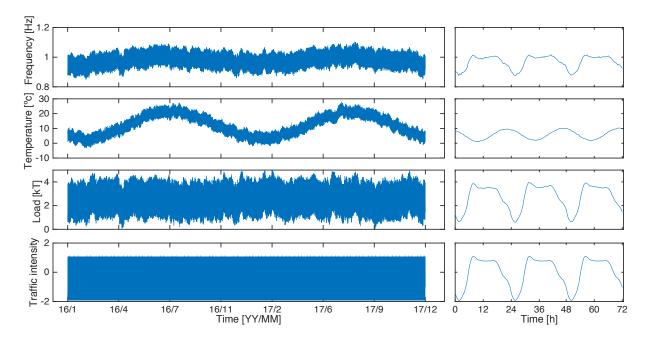

Figure 3: Simulated data for the illustrative example. The left graphs represent the entire two years dataset and the right graphs represent only the first three days.

observations is detailed below. Note that the superscript nomenclature follows: $(^{\mathrm{T}})$ temperature, $(^{\mathrm{P}})$ traffic pattern, $(^{\mathrm{L}})$ traffic load, and $(^{\mathrm{B}})$ frequencies. Also, following the nomenclature presented in Section 2.2: $(^{\mathrm{LL}})$ local level, $(^{\mathrm{S}})$ cyclic component, $(^{\mathrm{AR}})$ autoregressive component, and $(^{\mathrm{R}})$ regression component.

Temperature – y_t^{T}

The simulated temperature observations y_t^{T} are obtained by superposing; the average temperature, daily ($p = 1$ day) and seasonal ($p = 365$ day) sinusoidal cycles,

an autoregressive (AR(1)) process, and measurement errors so that

$$y_t^{\text{T}} = x_t^{\text{T,LL}} + x_t^{\text{T}_1,\text{S}_1} + x_t^{\text{T}_2,\text{S}_1} + x_t^{\text{T,AR}} + v_t^{\text{T}} \tag{9}$$

where each component is defined following

$$
\begin{aligned}
x_t^{\text{T,LL}} &= 12\,^{\circ}C && \text{(average temperature)}\\[4pt]
x_t^{\text{T}_1,\text{S}_1} &= 4\sin\left(\tfrac{2\pi}{1}\left(\tfrac{t}{48}+\tfrac{8}{24}\right)\right) && \text{(daily cycle)}\\[4pt]
x_t^{\text{T}_2,\text{S}_1} &= 9\sin\left(\tfrac{2\pi}{365}\left(\tfrac{t}{48}+\tfrac{8}{12}\cdot 365\right)\right) && \text{(seasonal cycle)}\\[4pt]
x_t^{\text{T,AR}} &= \underbrace{0.995}_{\phi^{\text{T,AR}}}\cdot x_{t-1}^{\text{T,AR}} + w_t^{\text{T,AR}}, \quad w_t^{\text{T,AR}}\sim\mathcal{N}(0,\underbrace{0.1}_{\sigma^{\text{T,AR}}}{}^2) && \text{(AR(1) process)}\\[4pt]
v_t^{\text{T}} &\sim \mathcal{N}(0,\underbrace{0.1}_{\sigma^{\text{T}}}{}^2) && \text{(measurement error)}
\end{aligned}
\tag{10}
$$

Traffic pattern – y_t^{P}

The traffic pattern describes the normalized traffic intensity. It is employed as a regression variable for defining the traffic load. The traffic pattern observations y_t^{P} are considered to be exacts and are defined following

$$y_t^{\text{P}} = x_t^{\text{P}} = h\left(\left(\tfrac{t}{48}-\left\lfloor\tfrac{t}{48}\right\rfloor\right)\cdot 24\right) \tag{11}$$

where $\lfloor\cdot\rfloor$ denotes the floor operator (i.e. round to the lowest integer), and $h(\cdot)$ is the normalized daily traffic intensity presented in Figure 4.
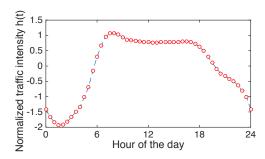

Figure 4: Syntetic data for daily traffic intensity

Load – $\mathbf{y}_t^{\text{L}}$

The load applied on the bridge is defined by superposing the average traffic load, the traffic intensity, which is a constant, time the traffic pattern, an autoregressive process, and observation errors, so that

$$y_t^{\text{L}} = x_t^{\text{L,LL}} + x_t^{\text{L|P,R}} + x_t^{\text{L,AR}} + v_t^{\text{L}} \tag{12}$$

where each component is defined following

$$
\begin{aligned}
x_t^{\text{L,LL}} &= 3\,kT & \text{(average traffic load)} \\[2mm]
x_t^{\text{L|P,R}} &= \underbrace{1.1}_{\phi^{\text{L|P,R}}} \cdot x_t^{\text{P}} & \text{(traffic intensity regression)} \\[2mm]
x_t^{\text{L,AR}} &= \underbrace{0.995}_{\phi^{\text{L,AR}}} \cdot x_{t-1}^{\text{L,AR}} + w_t^{\text{L,AR}}, \quad w_t^{\text{L,AR}} \sim \mathcal{N}(0, \underbrace{0.025^2}_{\sigma^{\text{L,AR}}}) & \text{(AR(1) process)} \\[2mm]
v_t^{\text{L}} &\sim \mathcal{N}(0, \underbrace{0.01^2}_{\sigma^{\text{L}}}) & \text{(measurement error)}
\end{aligned}
\tag{13}
$$

Frequencies – y_t^{B}

Frequency observations are simulated by superposing the baseline level of $1\,\text{Hz}$, the effect of traffic loading on the frequency, the effect of temperature on frequency, an autoregressive component, and observation errors. Frequency observations are defined by

$$y_t^{\text{B}} = x_t^{\text{B,LL}} + x_t^{\text{B|L,R}} + x_t^{\text{B|T,R}} + x_t^{\text{B,AR}} + v_t^{\text{B}} \tag{14}$$

where each component is defined following

$$
\begin{aligned}
x_t^{\text{B,LL}} &= 1\,\text{Hz} & \text{(average frequency)} \\[2mm]
x_t^{\text{B|L,R}} &= \underbrace{0.05}_{\phi^{\text{B|L,R}}}(x_t^{\text{L|P,R}} + x_t^{\text{L,AR}}) & \text{(traffic load regression)} \\[2mm]
x_t^{\text{B|T,R}} &= \underbrace{0.0029}_{\phi^{\text{B|T,R}}}\left(x_t^{\text{T}_1,\text{S}_1} + x_t^{\text{T}_2,\text{S}_1} + x_t^{\text{T,AR}}\right) & \text{(temperature regression)} \\[2mm]
x_t^{\text{B,AR}} &= \underbrace{0.995}_{\phi^{\text{B,AR}}} \cdot x_{t-1}^{\text{B,AR}} + w_t^{\text{B,AR}}, \quad w_t^{\text{B,AR}} \sim \mathcal{N}(0, \underbrace{0.0005^2}_{\sigma^{\text{B,AR}}}) & \text{(AR(1) process)} \\[2mm]
v_t^{\text{B}} &\sim \mathcal{N}(0, \underbrace{0.0025^2}_{\sigma^{\text{B}}}) & \text{(measurement error)}
\end{aligned}
\tag{15}
$$

14

5.2 BDLM construction

The BMLM takes the form expressed in Equations 1 and 2 where the global matrices defining the model are

$$
\begin{aligned}
\mathbf{y}_t &= [y_t^{\mathrm{B}}, y_t^{\mathrm{T}}, y_t^{\mathrm{L}}, y_t^{\mathrm{P}}]^{\mathsf{T}} \\
\mathbf{x}_t &= [\mathbf{x}_t^{\mathrm{B}}, \mathbf{x}_t^{\mathrm{T}}, \mathbf{x}_t^{\mathrm{L}}, x_t^{\mathrm{P}}]^{\mathsf{T}} \\
\mathbf{A}_t &= \mathrm{block\,diag}\,(\mathbf{A}_t^{\mathrm{B}}, \mathbf{A}_t^{\mathrm{T}}, \mathbf{A}_t^{\mathrm{L}}, A_t^{\mathrm{P}}) \\
\mathbf{C}_t &= \mathrm{block\,diag}\,(\mathbf{C}_t^{\mathrm{B}}, \mathbf{C}_t^{\mathrm{T}}, \mathbf{C}_t^{\mathrm{L}}, C_t^{\mathrm{P}}) \\
\mathbf{R}_t &= \mathrm{block\,diag}\,(R_t^{\mathrm{B}}, R_t^{\mathrm{T}}, R_t^{\mathrm{L}}, R_t^{\mathrm{P}}) \\
\mathbf{Q}_t &= \mathrm{block\,diag}\,(\mathbf{Q}_t^{\mathrm{B}}, \mathbf{Q}_t^{\mathrm{T}}, \mathbf{Q}_t^{\mathrm{L}}, Q_t^{\mathrm{P}})
\end{aligned}
$$

where each component of these model matrices is defined below. Complete matrices are presented in Appendix A. Model parameters to be estimated are regrouped in the set

$$
\mathcal{P} = \{\underbrace{\phi^{\mathrm{B|L,R}}, \phi^{\mathrm{B|T,R}}, \phi^{\mathrm{B|P,R}}, \phi^{\mathrm{L|P,R}}}_{\text{regression coefficients}}, \underbrace{\phi^{\mathrm{B,AR}}, \phi^{\mathrm{T,AR}}, \phi^{\mathrm{L,AR}}}_{\text{autocorr. coefficients}}, \underbrace{\sigma^{\mathrm{B,AR}}, \sigma^{\mathrm{L,AR}}, \sigma^{\mathrm{T,AR}}}_{\sqrt{\text{autocorr. variance}}}\}.
$$

Note that all local level standard deviations, $\sigma^{\mathrm{B,LL}} = \sigma^{\mathrm{L,LL}} = \sigma^{\mathrm{T,LL}} \equiv 0$ because the structure behavior, the temperature and the load are stationary.

Temperature – y_t^{T}

There are four components involved in the temperature model: (1) a local level, (2-3) two periodic signals with a period of one day ($\omega^{\mathrm{T1}} = \frac{2\pi}{48}$) and 365 days ($\omega^{\mathrm{T2}} = \frac{2\pi}{365\cdot48}$), (4) an autoregressive process. The vector of hidden state variables for the temperature is

$$
\mathbf{x}_t^{\mathrm{T}} = [\ \underbrace{x_t^{\mathrm{T,LL}}}_{\text{local level}}, \underbrace{x_t^{\mathrm{T1,S1}}, x_t^{\mathrm{T1,S2}}}_{\text{cycle, } p=1\,\text{day}}, \underbrace{x_t^{\mathrm{T2,S1}}, x_t^{\mathrm{T2,S2}}}_{\text{cycle, } p=365\,\text{day}}, \underbrace{x_t^{\mathrm{T,AR}}}_{\text{AR process}}\ ]
$$

where the ordering of each component remains the same for other matrices $\mathbf{C}_t^{\mathrm{T}}$, $\mathbf{A}_t^{\mathrm{T}}$ and $\mathbf{Q}_t^{\mathrm{T}}$. The observation matrix is defined following

$$
\mathbf{C}_t^{\mathrm{T}} = [1, 1, 0, 1, 0, 1]
$$

where the zeros indicate that components $x_t^{\mathrm{T1,S2}}$ and $x_t^{\mathrm{T2,S2}}$ do not contribute to the temperature observations. The measurement noise variance is $R_t^{\mathrm{T}} = (\sigma_{\mathrm{T}})^2$. The transition matrix is

$$
\mathbf{A}_t^{\mathrm{T}} = \mathrm{block\,diag}\left(1, \begin{bmatrix} \cos\omega^{\mathrm{T1}} & \sin\omega^{\mathrm{T1}} \\ -\sin\omega^{\mathrm{T1}} & \cos\omega^{\mathrm{T1}} \end{bmatrix}, \begin{bmatrix} \cos\omega^{\mathrm{T2}} & \sin\omega^{\mathrm{T2}} \\ -\sin\omega^{\mathrm{T2}} & \cos\omega^{\mathrm{T2}} \end{bmatrix}, \phi^{\mathrm{T,AR}}\right).
$$

The model error covariance is

$$\mathbf{Q}_t^{\mathrm{T}} = \operatorname{block\,diag}\left(0, 0, 0, (\sigma^{\mathrm{T,AR}})^2\right).$$

Traffic pattern – y_t^{P}

The traffic pattern observations y_t^{P} are exact so that the transition model A_t^{P} should bear no weight during the estimation. This is acheived by using an observation variance tending to zero and a model error variance tending to infinity. With these values, the Kalman gain tends to one, so that all the weight is put on the observation rather than on the model. This strategy is employed so that the other components in the BDLM can directly be modelled as a function of the traffic pattern observations. Matrices defining the traffic pattern component are

$$\mathbf{x}_t^{\mathrm{P}} = x_t^{\mathrm{P}} = y_t^{\mathrm{P}}, \ A_t^{\mathrm{P}} = 1, \ R_t^{\mathrm{P}} \to 0, \ Q_t^{\mathrm{T}} \to \infty$$

Traffic load – y_t^{L}

There are two independent components involved in the traffic load: (1) a local level and (2) an autoregressive process. There is also one dependent component, a regression component linking the traffic pattern to the traffic load. The vector of state variables for the traffic load is

$$\mathbf{x}_t^{\mathrm{L}} = [\ \underbrace{x_t^{\mathrm{L,LL}}}_{\text{local level}}, \ \underbrace{x_t^{\mathrm{L,AR}}}_{\text{AR process}}\ ]$$

where the ordering of each component remains the same for other matrices $\mathbf{C}_t^{\mathrm{L}}$, $\mathbf{A}_t^{\mathrm{L}}$ and $\mathbf{Q}_t^{\mathrm{L}}$. The observation matrix is $\mathbf{C}_t^{\mathrm{L}} = [1, 1]$, the measurement noise variance is $R_t^{\mathrm{L}} = (\sigma_{\mathrm{L}})^2$, the transition matrix is $\mathbf{A}_t^{\mathrm{L}} = \operatorname{block\,diag}(1, \phi^{\mathrm{L,AR}})$ and the model error covariance is $\mathbf{Q}_t^{\mathrm{L}} = \operatorname{block\,diag}(0, (\sigma^{\mathrm{L,AR}})^2)$. The dependent component is taken into account by introducing a regression coefficient in the global observation matrix

$$[\mathbf{C}_t]_{3,11} = \phi^{\mathrm{L|P,R}}.$$

This includes the effect of the traffic pattern in the traffic load observation. Note that the position $(3, 11)$ in the global observation matrix is defined by the ordering chosen for state variables.

Frequency – y_t^{B}

There are two independent components involved in the frequency: (1) a local level and (2) an autoregressive process. There are also five dependent components: (3-8) the five regression components respectively describe the dependency between the

16

frequency and temperature or traffic components. The vector of state variables for the frequency is

$$\mathbf{x}_t^{\text{B}} = [\underbrace{x_t^{\text{B,LL}}}_{\text{local level}}, \underbrace{x_t^{\text{B,AR}}}_{\text{AR process}}]$$

where the ordering of each component remains the same for other matrices $\mathbf{C}_t^{\text{B}}$, $\mathbf{A}_t^{\text{B}}$ and $\mathbf{Q}_t^{\text{B}}$. The observation matrix is $\mathbf{C}_t^{\text{B}} = [1, 1]$, the transition matrix is $\mathbf{A}_t^{\text{B}} = \text{block diag}\,(1, \phi^{\text{B,AR}})$ model error covariance is $\mathbf{Q}_t^{\text{T}} = \text{block diag}\,(0, (\sigma^{\text{B,AR}})^2)$. The dependent components are taken into account by introducing regression coefficients in the global observation matrix where,

$$[\mathbf{C}_t]_{1,11} = \phi^{\text{B|P,R}}, \;\; [\mathbf{C}_t]_{1,10} = \phi^{\text{B|L,R}}, \;\; [\mathbf{C}_t]_{1,4} = [\mathbf{C}_t]_{1,6} = [\mathbf{C}_t]_{1,8} = \phi^{\text{B|T,R}}$$

so that the effect of temperature and traffic pattern is included in the frequency observation. The measurement noise variance is assumed to be known $R_t^{\text{B}} = (\sigma_{\text{B}})^2$. In practice, methods such as the one proposed by Yuen and Kuok [33] can be employed for estimating this parameters.

Graphical model representation

The BDLM defined in Section 5.2 can be represented by a graphical model as described in Section 2.3. Figure 5 presents one time-slice from the Dynamic Bayesian Network (i.e. graphical model) describing the BDLM. This figure regroups all components presented above in Section 5.2.

5.3   Computational efficiency

It takes approximately 0.0008 second to run one time-slice of the U-D filter on a laptop computer, and it takes approximately 15 seconds to process one year worth of data (for a sampling period of 30 minutes). For the same configuration, it takes approximately 0.0005 second per time slice with the standard Kalman filter presented in Section 3. Only the U-D filter formulation is employed in this paper because, even if the Kalman filter is faster, it leads to several numerical inaccuracies invalidating the final results. However, note that both the U-D and Kalman filters are estimating the exact same quantities and have the same physical interpretation. With either the U-D of the Kalman filter, a single off-the-shelf computer would be able to process in real-time, the data from thousands of sensors which would be positioned across a population of structures.

5.4   Model parameter estimation

A training period of *six months* is employed to learn model parameters $\mathcal{P}$. This duration is chosen because it displays the full amplitude of the seasonal temperature
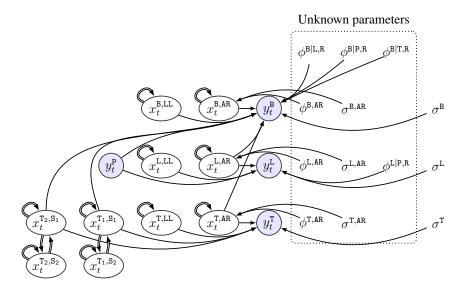
Figure 5: Graphical model (i.e. Dynamic Bayesian network) representing the causal dependencies between each component of the model. Circles represent random variables; links correspond to causal relations; double-line links are a shorthand notation for links between time steps. Nodes without a border represent deterministic parameters; color-filled nodes correspond to *observed variables*; white-filled nodes correspond to *unobserved/hidden variables*.

(January-June). Note that without the effect of seasonal temperature, a shorter training period could be selected. The initial state $\mathbf{x}_0$ is described by a broad (i.e. non-informative) prior where each component has a mean of $[\boldsymbol{\mu_0}]_i = 0, \forall i$ and a covariance $[\boldsymbol{\Sigma_0}]_{ii} = 10^6, \forall i$, $[\boldsymbol{\Sigma_0}]_{ij} = 0, \forall i \neq j$.

In order to establish a reference, the matrix-wise EM algorithm is first employed while starting from the true parameter values. In this configuration, the EM algorithm converges to parameter values that are negligibly close to the true values. The log-likelihood of this set of reference parameters is -3434. Note that although the initial state $\mathbf{x}_0$ can be identified at the same time as other unknown parameters, it has been chosen to keep them as a broad prior in order to illustrate how information about the hidden states is gained during the training period.

In a second step, a realistic scenario is tested where 10 sets of initial parameter values are generated from a Gaussian distribution centred on true parameter values and with a coefficient of variation of 1. The EM algorithm is employed iteratively (≈ 7 sec./evaluation) either until reaching 500 evaluations, or when the difference in the likelihood between two consecutive time steps is below 10^{-5}. Note that during the initial perturbation and optimization steps, parameter values are constrained to their feasible domain: $\mathbb{R}^+$ for variances (σ^2), $(0, 1)$ for the AR coefficients $\phi^{\mathtt{AR}}$,

and $\mathbb{R}$ for the regression coefficients $\phi^{i|j}$.

Figure 6a presents the evolution of the log-likelihood for the starting point having led to the highest log-likelihood (-3379) and the estimated parameter values

$$\mathcal{P}^* = \{0.0501, 0.0030, 0.0539, 1.0780, 0.9964, 0.9934, 0.9935, 0.0005, 0.0100, 0.0994\}.$$

Figure 6b presents the evolution of the relative error in the parameter values. The absolute relative difference between the true parameter values and $\mathcal{P}^*$ is at most 2.8% with a mean of 0.25%. In order to be representative of real situations where the true values remain unknown, all the following results are calculated using the parameter values $\mathcal{P}^*$ instead of the true values.
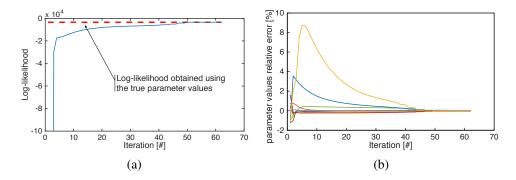

(a) (b)

Figure 6: a) Evolution of the log-likelihood with the number of EM iterations for the best starting point that has led to the model parameter $\mathcal{P}^*$. b) Evolution of the relative error between true and parameter values. The right most values in (b) represent the relative discrepancy between the true parameter values and $\mathcal{P}^*$.

5.4.1 Model components separation

The BDLM is employed to separate the observed signal into its hidden components. The filtered signals $\mathbf{y}_{1:T}$ along with selected hidden components are presented in Figures 7-9 where all left graphs present the entire dataset (2 years) and the right graphs present the last two weeks. Note that $x_t^{\text{T1,S2}}$ and $x_t^{\text{T2,S2}}$ are not presented because they do not directly contribute to the filtered signal $\mathbf{y}_{1:T}^{\text{T}}$. The load pattern regressor $\mathbf{y}_{1:T}^{\text{P}}$ is also omitted because it consists of exact quantities. The narrow $\pm\sigma$ interval around the mean values in Figures 7-9 show that the BDLM is able to separate the raw datasets representing structural responses and external effects into its components. On these figures, we can see how in approximately five months, the BDLM has gone from a broad prior for the hidden state to precise estimations of the true states.

19

(a) Local level $x_t^{\text{B,LL}}$

(b) AR process $x_t^{\text{B,AR}}$

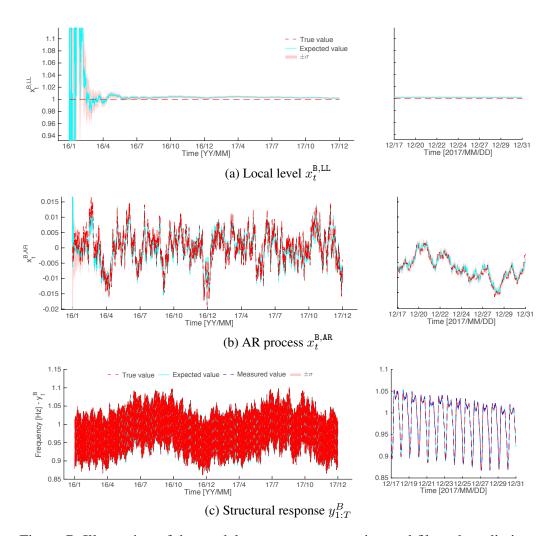(c) Structural response $y_{1:T}^{B}$

Figure 7: Illustration of the model component separation and filtered predictions for the structural response. All left graphs present the entire dataset (2 years) and the right graphs present the last two weeks

(a) Local level $x_t^{\text{T,LL}}$

(b) Daily cycle $x_t^{\text{T1,S1}}$

(c) Seasonal cycle $x_t^{\text{T2,S1}}$

(d) AR process $x_t^{\text{T,AR}}$
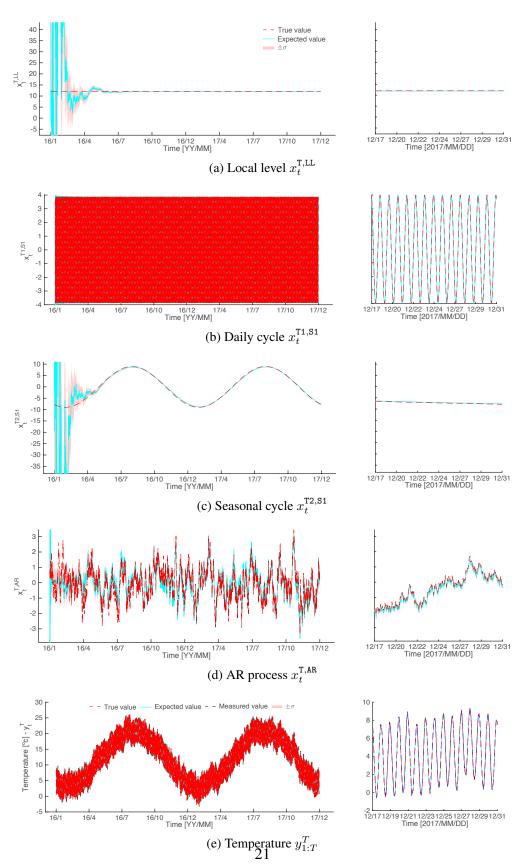
(e) Temperature $y_{1:T}^{T}$

21

Figure 8: Illustration of the model component separation and filtered predictions
for the temperature. All left graphs present the entire dataset (2 years) and the right
graphs present the last two weeks.

(a) Local level $x_t^{\text{L,LL}}$

(b) AR process $x_t^{\text{L,AR}}$
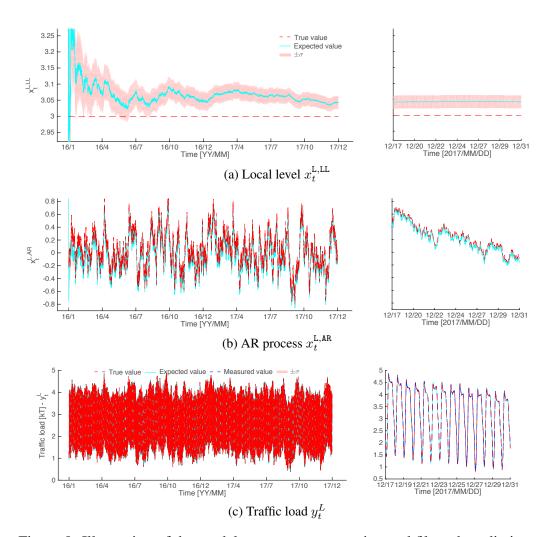
(c) Traffic load y_t^L

Figure 9: Illustration of the model component separation and filtered predictions for the traffic load. All left graphs present the entire dataset (2 years) and the right graphs present the last two weeks.

Note that temperature and traffic loads are decomposed into their respective components not because they are themselves interesting, but because the frequency response depends on these components.

5.4.2 Handling of missing data and outliers

This section presents how the BDLM is handling two common situations in SHM without requiring any modifications or special treatement. It first shows how the BDLM can fill the gap when structural responses and external effects data are missing. Figure 10 presents the filtered signal for the last two weeks of the dataset where seven days of data are missing. The filtered signal is only marginally affected by missing data through an augmentation of the uncertainty in the AR process. Because $\phi^{\text{B,AR}} < 1$, when data is missing, the AR process tends to its zero-mean stationary state. When data is made available again, the estimation quickly returns to an accurate and precise estimation of the true hidden state.

(a) Local level $x_t^{\text{B,LL}}$

(b) AR process $x_t^{\text{B,AR}}$

(c) Structural response $y_{1:T}^B$
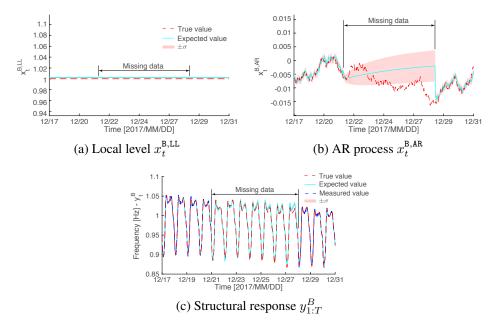
Figure 10: Example of results in the presence of missing data for the structural responses.

Figure 11 presents the effect of having outliers corrupting the measured structural responses. In practical situations, outliers having unreasonable values are easy to identify and remove using thresholds. Outliers that are in a gray-zone where they are at the same time unlikely, yet possible are the most problematic. BDLM is capable of handling those outliers in a seamless manner because filtering combines

(a) Local level $x_t^{\text{B,LL}}$

(b) AR process $x_t^{\text{B,AR}}$

(c) Structural response $y_{1:T}^B$

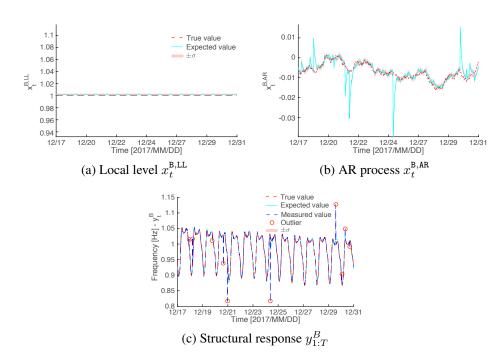Figure 11: Example of results in the presence of outliers for the structural responses. In (c), outliers are indicated by a circle.

24

observations with a transition model. In this case, outliers introduce biases in the estimation of the AR process. Yet, the estimates of the local level representing the baseline behavior of the structure remains unaffected by the presence of outliers.

6 Conclusion

This paper presents a framework for building, learning and estimating Bayesian Dynamic Linear Models (BDLM). Specifically, the contributions of this paper enable creating models of external effect and structural responses by superposing generic components, i.e. baseline response, periodic cycles, autoregressive components and regression components. The framework proposed offers robustness to numerical errors, outliers and missing data. The EM calibration strategy has been shown to enable the quick estimation of unknown parameters. Moreover, it is compatible with non-uniform time steps which are common in practice.

Note that although the method proposed in this paper is able to handle multiple structural responses simultaneously, in practice this would require special considerations regarding the definition of the model error covariance matrix. The study of this special case is beyond the scope of this paper.

The BDLM has the potential to enable a widespread application of SHM because (i) with minimal effort, it can be adapted to any type of structures, (ii) it can process in real-time, on a single desktop computer, the data acquired on thousands of structures and learn the model parameters. The BDLM presented in this paper is the first necessary step toward more advanced methods that will perform real-time autonomous anomaly detection.

7 Acknowledgements

References

[1] G. Bartram and S. Mahadevan. Integration of heterogeneous information in shm models. *Structural Control and Health Monitoring*, 2013.

[2] D. Bernal, D. Zonta, and M. Pozzi. Arx residuals in damage detection. *Structural Control and Health Monitoring*, 19(4):535–547, 2012.

[3] G. Bierman and C. Thornton. Numerical comparison of kalman filter algorithms: Orbit determination case study. *Automatica*, 13(1):23–35, 1977.

[4] F. Casciati and L. Faravelli. Sensor placement driven by a model order reduction (mor) reasoning. *Smart Structures and Systems*, 13(3):343–352, 2014.

[5] M. Chang and S. N. Pakzad. Observer kalman filter identification for output-only systems using interactive structural modal identification toolsuite. *Journal of Bridge Engineering*, 2013.

[6] Y. Chen and M. Feng. Structural health monitoring by recursive Bayesian filtering. *Journal of Engineering Mechanics*, 135(4):231–242, 2009.

[7] S. Cho, R. K. Giles, and B. F. Spencer. System identification of a historic swing truss bridge using a wireless sensor network employing orientation correction. *Structural Control and Health Monitoring*, 2014.

[8] Z. Dzunic, J. G. Chen, H. Mobahi, O. Buyukozturk, and J. W. Fisher III. A bayesian state-space approach for damage detection and classification. In *Dynamics of Civil Structures, Volume 2*, pages 171–183. Springer, 2015.

[9] L. Faravelli and S. Casciati. Structural damage detection and localization by response change diagnosis. *Progress in Structural Engineering and Materials*, 6(2):104–115, 2004.

[10] C. Farrar, G. Park, D. Allen, and M. Todd. Sensor network paradigms for structural health monitoring. *Structural control and health monitoring*, 13(1):210–225, 2006.

[11] C. Farrar and K. Worden. *Structural Health Monitoring: A Machine Learning Perspective*. John Wiley & Sons, 2012.

[12] A. Gelman, J. B. Carlin, H. S. Stern, and D. B. Rubin. *Bayesian data analysis*. CRC Press, 3 edition, 2014.

[13] Z. Ghahramani and G. E. Hinton. Parameter estimation for linear dynamical systems. Technical Report CRG-TR-96-2, University of Toronto, Dept. of Computer Science, 1996.

[14] B. P. Gibbs. *Advanced Kalman filtering, least-squares and modeling: a practical handbook*. John Wiley & Sons, 2011.

[15] E. Hernandez. Optimal model-based state estimation in mechanical and structural systems. *Structural Control and Health Monitoring*, 20(4):532–543, 2013.

[16] K. Mehrotra and P. R. Mahapatra. A jerk model for tracking highly maneuvering targets. *Aerospace and Electronic Systems, IEEE Transactions on*, 33(4):1094–1105, 1997.

[17] H.-Q. Mu and K.-V. Yuen. Novel outlier-resistant extended kalman filter for robust online structural identification. *Journal of Engineering Mechanics*, 141(1):DOI: 10.1061/(ASCE)EM.1943–7889.0000810, 2015.

[18] K. Murphy. *Machine learning: a probabilistic perspective*. The MIT Press, 2012.

[19] K. P. Murphy. Switching kalman filters. Technical report, Citeseer, 1998.

[20] P. Omenzetter and J. M. W. Brownjohn. Application of time series analysis for bridge monitoring. *Smart Materials and Structures*, 15(1):129–138, 2006.

[21] J. Pearl. *Probabilistic reasoning in intelligent systems: networks of plausible inference*. Morgan Kaufmann, San Mateo, USA, 1988.

[22] R. Prado and M. West. *Time series: modeling, computation, and inference*. CRC Press, 2010.

[23] D. Simon. *Optimal state estimation: Kalman, H infinity, and nonlinear approaches*. Wiley, 2006.

[24] A. Smyth and M. Wu. Multi-rate kalman filtering for the data fusion of displacement and acceleration response measurements in dynamic system monitoring. *Mechanical Systems and Signal Processing*, 21(2):706–723, 2007.

[25] H. Sohn, C. R. Farrar, N. F. Hunter, and K. Worden. Structural health monitoring using statistical pattern recognition techniques. *Transactions-American Society of Mechanical Engineers Journal of Dynamic Systems Measurement And Control*, 123(4):706–711, 2001.

[26] I. Solhjell. Bayesian forecasting and dynamic models applied to strain data from the göta river bridge. Master's thesis, University of Oslo, 2009.

[27] H. Sun, D. Feng, Y. Liu, and M. Q. Feng. Statistical regularization for identification of structural parameters and external loadings using state space models. *Computer-Aided Civil and Infrastructure Engineering*, 30(11):843–858, 2015.

[28] F. Vicario, M. Q. Phan, R. Betti, and R. W. Longman. Output-only observer/kalman filter identification (o3kid). *Structural Control and Health Monitoring*, 22(5):847–872, 2015.

[29] M. West. Bayesian dynamic modelling. *Bayesian Inference and Markov Chain Monte Carlo: In Honour of Adrian FM Smith*, pages 145–166, 2013.

[30] M. West and J. Harrison. *Bayesian Forecasting and Dynamic Models*. Springer Series in Statistics. Springer New York, 1999.

[31] K. Yuen. *Bayesian methods for structural dynamics and civil engineering*. Wiley, 2010.

[32] K.-V. Yuen and S.-C. Kuok. Modeling of environmental influence in structural health assessment for reinforced concrete buildings. *Earthquake Engineering and Engineering Vibration*, 9(2):295–306, 2010.

[33] K.-V. Yuen and S.-C. Kuok. Online updating and uncertainty quantification using nonstationary output-only measurement. *Mechanical Systems and Signal Processing*, 66:62–77, 2016.

[34] P. Zarchan and H. Musoff. *Fundamentals of Kalman filtering: a practical approach*, volume 208. Aiaa, 2005.

[35] H. Zheng and A. Mita. Damage indicator defined as the distance between arma models for structural health monitoring. *Structural control & health monitoring*, 15(7):992, 2008.

Appendix A

The complete vector of *state variables* ($\mathbf{x}_t$), the model *transition matrix* ($\mathbf{A}_t$), the model *observation matrix* ($\mathbf{C}_t$), the model *observation error covariance matrix* ($\mathbf{R}_t$) and, the model *model error covariance matrix* ($\mathbf{Q}_t$) are presented below

$$\mathbf{x}_t = [x_t^{\mathrm{B,LL}}, x_t^{\mathrm{B,AR}}, x_t^{\mathrm{T,LL}}, x_t^{\mathrm{T1,S1}}, x_t^{\mathrm{T1,S2}}, x_t^{\mathrm{T2,S1}}, x_t^{\mathrm{T2,S2}}, x_t^{\mathrm{T,AR}}, x_t^{\mathrm{T,LL}}, x_t^{\mathrm{L,AR}}, x_t^{\mathrm{P}}]^{\mathsf{T}}$$

$$\mathbf{A}_t = \begin{bmatrix}
1 & 0 & 0 & 0 & 0 & 0 & 0 & 0 & 0 & 0 & 0 \\
0 & \phi^{\mathrm{B,AR}} & 0 & 0 & 0 & 0 & 0 & 0 & 0 & 0 & 0 \\
0 & 0 & 1 & 0 & 0 & 0 & 0 & 0 & 0 & 0 & 0 \\
0 & 0 & 0 & \cos\omega^{\mathrm{T1}} & \sin\omega^{\mathrm{T1}} & 0 & 0 & 0 & 0 & 0 & 0 \\
0 & 0 & 0 & -\sin\omega^{\mathrm{T1}} & \cos\omega^{\mathrm{T1}} & 0 & 0 & 0 & 0 & 0 & 0 \\
0 & 0 & 0 & 0 & 0 & \cos\omega^{\mathrm{T2}} & \sin\omega^{\mathrm{T2}} & 0 & 0 & 0 & 0 \\
0 & 0 & 0 & 0 & 0 & -\sin\omega^{\mathrm{T2}} & \cos\omega^{\mathrm{T2}} & 0 & 0 & 0 & 0 \\
0 & 0 & 0 & 0 & 0 & 0 & 0 & \phi^{\mathrm{T,AR}} & 0 & 0 & 0 \\
0 & 0 & 0 & 0 & 0 & 0 & 0 & 0 & 1 & 0 & 0 \\
0 & 0 & 0 & 0 & 0 & 0 & 0 & 0 & 0 & \phi^{\mathrm{L,AR}} & 0 \\
0 & 0 & 0 & 0 & 0 & 0 & 0 & 0 & 0 & 0 & 1
\end{bmatrix}$$

$$\mathbf{C}_t = \begin{bmatrix}
1 & 1 & 0 & \phi^{\mathrm{B|T,R}} & 0 & \phi^{\mathrm{B|T,R}} & 0 & \phi^{\mathrm{B|T,R}} & 0 & \phi^{\mathrm{B|L,R}} & \phi^{\mathrm{B|P,R}} \\
0 & 0 & 1 & 1 & 0 & 1 & 0 & 1 & 0 & 0 & 0 \\
0 & 0 & 0 & 0 & 0 & 0 & 0 & 0 & 1 & 1 & \phi^{\mathrm{L|P,R}} \\
0 & 0 & 0 & 0 & 0 & 0 & 0 & 0 & 0 & 0 & 1
\end{bmatrix}$$

$$\mathbf{R}_t = \begin{bmatrix}
(\sigma_{\mathrm{B}})^2 & 0 & 0 & 0 \\
0 & (\sigma_{\mathrm{T}})^2 & 0 & 0 \\
0 & 0 & (\sigma_{\mathrm{L}})^2 & 0 \\
0 & 0 & 0 & \to 0
\end{bmatrix}$$

$$\mathbf{Q}_t = \text{block diag}\left(0, (\sigma^{\mathrm{B,AR}})^2, 0, 0, 0, 0, 0, (\sigma^{\mathrm{T,AR}})^2, 0, (\sigma^{\mathrm{L,AR}})^2, \to \infty\right)$$